The following supplements accompany the article

On-shelf larval retention limits population connectivity in a coastal broadcast spawner

Peter R. Teske, Jonathan Sandoval-Castillo, Erik van Sebille, Jonathan Waters, Luciano B. Beheregaray*

*Corresponding author: luciano.beheregaray@flinders.edu.au

Marine Ecology Progress Series 532: 1–12 (2015)

Supplement 1: Supplementary Methods

Spatial autocorrelation. A correlation coefficient (*r*) was estimated between categories of geographic distance and the mean pairwise genetic distances between individuals in each category. Statistical significance was tested using 1,000 permutations to estimate a 95% confidence interval about the null hypothesis of no spatial genetic structure. Values of *r* that are beyond this confidence interval are considered to be significantly different. We also estimated 95% confidence intervals around *r*. We then performed a number of spatial autocorrelation analyses with different size classes and presented correlograms for distance class sites 100 km and 1200 km (see 'Results' in the main article). Given the arbitrary choice of distance class, which may not necessarily reveal the true extent of non-random genetic structure (Escudero et al. 2003), we explored the effect of cumulatively increasing geographic distance class sizes (by increments of 100 km) on *r* as a means of determining the maximum distance class at which departures from random dispersal can be identified.

Seascape Genetics: Genetic vs. environmental data. Geographic distances were measured as the minimum coastline distances between each pair of sampling localities using ARCMAP 10.1 (Environmental Systems Research Institute, Redlands, CA). Thermal gradients were analysed using data on sea surface temperatures from the last 100 years obtained from the NOAA World Ocean Data Base

(http://www.nodc.noaa.gov/OC5/SELECT/dbsearch/dbsearch.html). We used ODV 4.5 (Schlitzer 2002) to extract the mean summer temperature, the mean annual temperature and the difference between minimum and maximum temperature (ΔT) at each locality. A thermal distance matrix was created by estimating absolute differences in temperature between pairs of localities, for both summer temperature and ΔT. Lastly, the effects of ocean circulation on genetic connectivity were explored using the Connectivity Modelling System v1.1 (Paris et al 2013) to integrate virtual Lagrangian particles within the Ocean General Circulation Model For the Earth Simulator (OFES; Masumoto et al. 2004) to estimate pairwise advection connectivity matrices. The OFES has a horizontal resolution of 1/10 ° and the Lagrangian particles were advected using the 2D velocity fields at 5 m depth and for the years 1980 to 2010. The OFES model has previously been shown to accurately reproduce the circulation in the Great Australian Bight (Van Sebille et al 2012). During the species' approximate spawning season (between 1 September and 30 January), ~350,000 particles were released per sampling locality (except at sites 7 and 9 because the resolution of our model did not allow separating them from sites 8 and 10, respectively) evenly spaced in a semicircle with 1° radius centered at the site coordinates. Particles were advected for 150 days (Model 1), and their location was recorded every hour, whereupon it was determined where each particle had settled; settlement was defined as the first time a particle location intersected with in the 1° semicircle of any sampling locality at least 90 days after larval release. For a second model (Model 2), which integrated a stepping-stone model of dispersal, we considered the simulation results of Model 1 as a single reproductive event (i.e. a single reproductive cycle, or spawning event, per year). Based on the number of locally retained (i.e., particles that settled in the same locality from which they were released) and imported particles (i.e., particles that arrived at a particular locality but originated from a different locality), we determined the origin composition of particles liberated in each locality for the next

reproductive event. For each pair of localities, particles that were released at one locality and arrived at another were considered to be migrants. Pairwise advection connectivity was defined as the total number of migrants between each pair of localities after four reproductive events (the mean number of reproductive events in which a particular individual will participate during its lifetime). As the number of migrants among pairs of localities differed by up to four orders of magnitude, we corrected these estimates for subsequent analyses by calculating their natural logarithm.

Supplement 2: Supplementary tables

Table S1. p-values of tests for Hardy-Weinberg equilibrium for each locus and site. Significance is shown as * ($p<0.05$) and ** ($p<0.01$).

	Locus												
Site	Neat01	Neat02	Neat03	Neat04	Neat05	Neat07	Neat09	Neat10	Neat12	Neat14	Neat16	Neat18	Neat19
1	0.040	0.498	0.837	0.583	0.075	0.000**	0.032*	0.857	0.296	0.516	0.016*	0.048	0.290
2	0.020*	0.340	0.571	0.264	0.186	0.314	0.250	0.627	0.553	0.159	0.260	0.028	0.325
3	0.043	0.121	0.141	0.021*	0.200	0.278	0.891	0.088	0.067	0.530	0.548	0.008**	0.303
4	0.043*	0.322	0.503	0.009**	0.455	0.618	0.371	0.903	0.659	0.729	0.462	0.076	0.708
5	0.816	0.559	0.259	0.922	0.497	0.288	0.361	0.372	0.365	0.265	0.458	0.002**	0.165
6	0.121	0.614	0.721	0.536	0.586	0.489	0.923	0.311	0.896	0.493	0.642	0.001**	0.423
7	0.033*	0.663	0.670	0.858	0.460	0.987	0.871	0.228	0.110	0.676	0.678	0.099	0.397
8	0.217	0.428	0.154	0.643	0.486	0.746	0.273	0.889	0.022*	0.899	0.622	0.001**	0.850
9	0.698	0.315	0.165	0.761	0.020*	0.503	0.884	0.837	0.582	0.411	0.003**	0.062	0.558
10	0.637	0.797	0.759	0.988	0.644	0.717	0.793	0.019*	0.969	0.975	0.551	0.000**	0.929
11	0.087	0.358	0.521	0.427	0.127	0.885	0.456	0.897	0.310	0.106	0.028*	0.006**	0.979
12	0.738	0.762	0.707	0.867	0.713	0.754	0.500	0.693	0.997	0.204	0.203	0.005**	0.803
13	0.173	0.575	0.789	0.704	0.233	0.127	0.522	0.835	0.319	0.701	0.926	0.067	0.300
14	0.408	0.644	0.962	0.908	0.062	0.697	0.082	0.547	0.483	0.371	0.425	0.095	0.501
15	0.001**	0.597	0.865	0.707	0.220	0.000**	0.290	0.000**	0.502	0.878	0.877	0.059	0.203
16	0.084	0.397	0.022*	0.992	0.177	0.011*	0.440	0.364	0.622	0.357	0.444	0.063	0.248
17	0.936	0.820	0.916	0.910	0.633	0.975	0.076	0.112	0.337	0.355	0.882	0.073	0.947
18	0.177	0.253	0.137	0.606	0.014*	0.264	0.041*	0.142	0.040*	0.944	0.002**	0.043*	0.746
19	0.424	0.513	0.237	0.964	0.337	0.362	0.229	0.183	0.754	0.084	0.001**	0.001*	0.227
20	0.519	0.267	0.280	0.332	0.189	0.493	0.398	0.253	0.781	0.770	0.001**	0.016*	0.515
21	0.204	0.411	0.670	0.368	0.195	0.485	0.076	0.173	1.000	0.030*	0.806	0.025*	0.851
% amplification	96.44	75.80	99.54	98.85	99.54	96.67	98.85	99.66	95.87	98.28	98.08	90.08	98.74

Table S2. Genetic differentiation between samples of *Nerita atramentosa* from 21 localities. F_{ST} values are shown below the diagonal and D_{est} values above the diagonal. Values in bold were significant after correction for multiple tests (adjusted p = 0.0137).

	1	2	3	4	5	6	7	8	9	10	11	12	13	14	15	16	17	18	19	20	21
1		**0.054**	**0.037**	**0.051**	0.025	**0.034**	0.024	**0.030**	**0.043**	**0.032**	**0.048**	**0.060**	**0.063**	**0.061**	0.009	0.019	**0.027**	**0.034**	**0.063**	**0.038**	**0.061**
2	**0.015**		0.008	0.010	0.020	**0.029**	0.028	0.013	0.003	0.019	0.012	0.008	0.024	**0.031**	**0.041**	0.027	0.022	0.012	0.021	0.001	**0.037**
3	**0.012**	0.008		0.016	0.006	0.018	0.016	0.016	0.003	0.005	0.007	0.007	0.008	0.006	0.020	0.013	0.003	0.009	0.021	0.004	**0.028**
4	**0.015**	0.009	0.008		0.012	0.009	0.008	0.001	0.000	0.019	0.022	0.008	**0.026**	**0.030**	**0.056**	**0.049**	0.023	**0.038**	**0.035**	0.010	**0.025**
5	0.011	0.010	0.007	0.009		0.019	0.012	0.000	0.006	0.015	**0.025**	0.023	**0.023**	0.023	**0.041**	0.017	0.008	0.000	0.024	0.001	0.015
6	**0.012**	**0.011**	0.008	0.008	0.009		0.002	0.004	0.000	0.014	**0.024**	0.006	0.014	0.018	**0.064**	**0.031**	0.024	0.023	**0.043**	**0.030**	**0.039**
7	0.011	0.012	0.009	0.008	0.009	0.007		0.000	0.016	0.011	0.017	0.010	0.027	**0.028**	**0.036**	0.020	0.015	0.021	0.019	0.009	0.016
8	**0.011**	0.009	0.008	0.007	0.006	0.007	0.007		0.000	0.008	0.022	0.019	**0.032**	**0.034**	**0.044**	0.025	0.001	0.010	0.023	0.000	0.012
9	**0.013**	0.007	0.006	0.006	0.007	0.005	0.009	0.006		0.008	0.019	0.001	0.015	0.009	**0.045**	**0.029**	0.011	0.018	0.017	0.000	**0.023**
10	**0.011**	0.009	0.006	0.009	0.008	0.008	0.008	0.007	0.006		0.012	0.021	0.019	**0.030**	0.021	0.016	0.013	0.019	0.019	0.010	0.024
11	**0.013**	0.009	0.006	0.009	**0.009**	**0.009**	0.009	0.009	0.008	0.007		0.016	0.019	0.010	**0.025**	**0.021**	0.016	0.022	0.018	0.002	**0.032**
12	**0.015**	0.008	0.006	0.007	0.009	0.007	0.008	0.008	0.005	**0.008**	0.008		0.004	0.011	**0.064**	**0.034**	0.020	0.016	**0.027**	0.020	**0.032**
13	**0.016**	0.010	0.006	**0.010**	0.009	0.008	**0.010**	**0.010**	0.007	**0.008**	0.008	0.006		0.012	**0.068**	**0.047**	**0.043**	0.014	**0.037**	**0.028**	**0.032**
14	**0.015**	**0.011**	0.006	**0.011**	0.009	0.008	0.010	**0.011**	0.007	**0.010**	0.007	0.007	0.007		**0.050**	**0.040**	0.010	0.021	**0.033**	0.016	0.021
15	0.008	**0.013**	0.008	**0.015**	**0.012**	**0.015**	**0.012**	**0.012**	**0.012**	0.009	**0.009**	**0.015**	**0.015**	**0.013**		0.020	0.021	**0.033**	**0.038**	0.019	**0.052**
16	0.010	0.011	0.008	**0.014**	0.009	**0.010**	0.010	0.010	**0.010**	0.008	0.009	**0.011**	**0.012**	**0.011**	0.009		0.000	0.015	0.011	0.008	**0.051**
17	**0.011**	0.010	0.006	0.010	0.008	0.009	0.009	0.006	0.007	0.008	0.008	0.009	**0.012**	0.007	0.009	0.006		0.019	0.017	0.000	0.011
18	**0.012**	0.009	0.007	**0.012**	0.007	0.010	0.010	0.008	0.009	0.009	0.009	0.008	0.008	0.009	**0.011**	0.009	0.009		0.021	0.008	**0.030**
19	**0.016**	0.010	0.009	**0.012**	0.010	**0.012**	0.009	0.009	0.008	0.008	0.008	**0.010**	**0.011**	**0.010**	**0.011**	0.008	0.009	0.009		0.000	**0.033**
20	**0.012**	0.008	0.006	0.008	0.007	**0.010**	0.008	0.006	0.006	0.007	0.006	0.008	**0.009**	0.008	0.008	0.007	0.005	0.008	0.006		0.007
21	**0.016**	**0.012**	**0.010**	0.010	0.009	**0.012**	0.009	0.008	**0.009**	**0.009**	**0.010**	**0.010**	**0.010**	0.009	**0.013**	**0.013**	0.008	**0.011**	**0.011**	0.007	

Table S3. Results of Spearman rank correlations performed on monthly data from the number of individuals that successfully settled at the coast versus the number of individuals that remained on the continental shelf.

Month	*R*	p
September	0.66	0.0015
October	0.74	0.0002
November	0.67	0.0013
December	0.61	0.0047
January	0.60	0.0048

Table S4. Results of Mantel tests between the matrices of explanatory variables, including coastal distance, inverse of advection connectivity and thermal distance.

Explanatory variables	Correlation	p	Variance explained (%)
Coastal Distance vs Advection Connectivity	0.9252	0.0005	85.6
Delta Temperature vs Advection Connectivity	-0.1717	0.0250	2.9
Delta Temperature vs Coastal Distance	-0.1773	0.0230	3.2

Supplement 3: Supplementary Figures

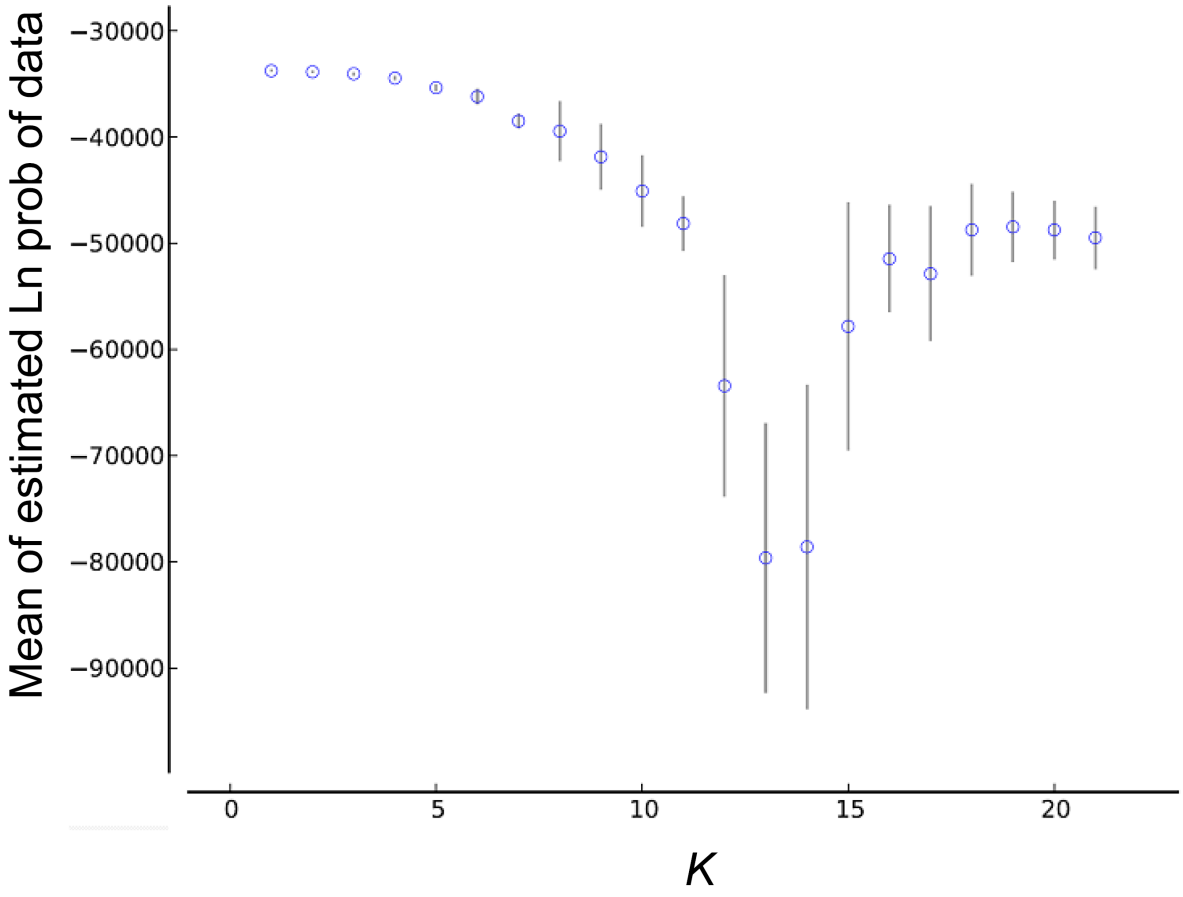

Fig. S1. Mean Ln probability of the data as a function of the number of population clusters (*K*) specified in STRUCTURE for the analyses of *Nerita atramentosa* microsatellite data.

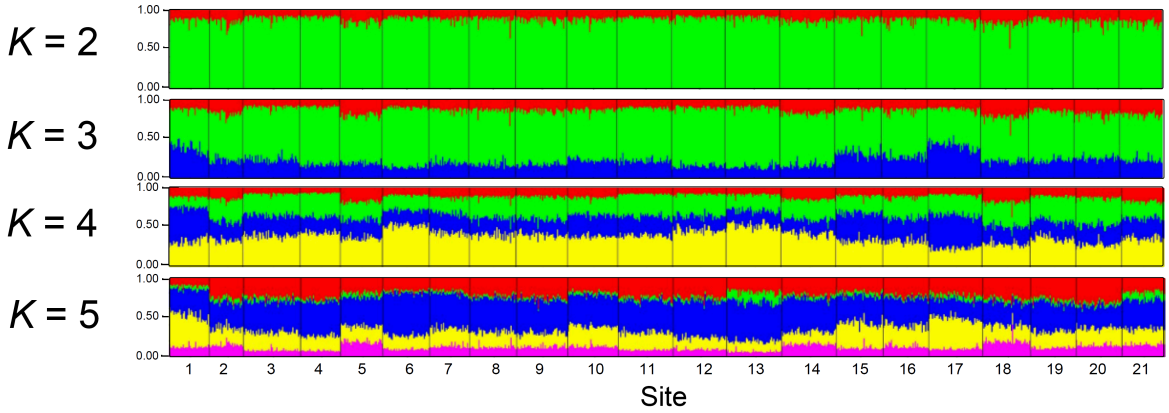

Fig. S2. STRUCTURE bar plots for *K*=2 to *K*=5 for 21 sites at which *Nerita atramentosa* was sampled.

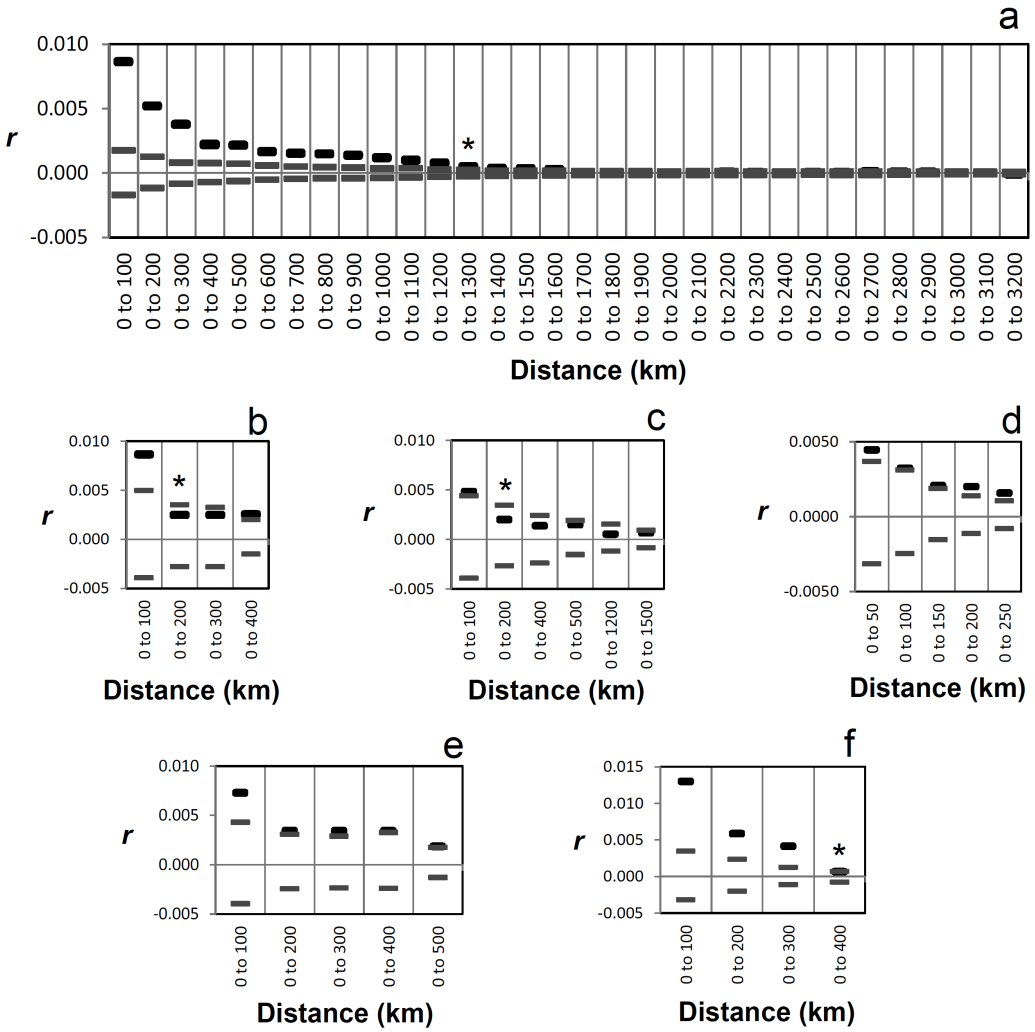

Fig. S3. Spatial autocorrelation analyses of *Nerita atramentosa*. Plots depict the autocorrelation coefficients of multilocus genotypes among individuals (*r*; black horizontal bars) at cumulatively increasing geographic distance class sizes (by increments of 50 or 100 km) for the following data sets: (a) all samples included; (b) sites 1-3 (LC region); (c) sites 3-6 (GAB); (d) sites 6-11 (South Australia); (e) sites 12, 18 and 19 (ZC region); (f) sites 13-17 (Bass Strait). Grey horizontal bars represent the 95% confidence intervals under the hypothesis of no spatial autocorrelation, and asterisks indicate at which distance class *r* was no longer significantly greater than the upper 95% confidence bound.

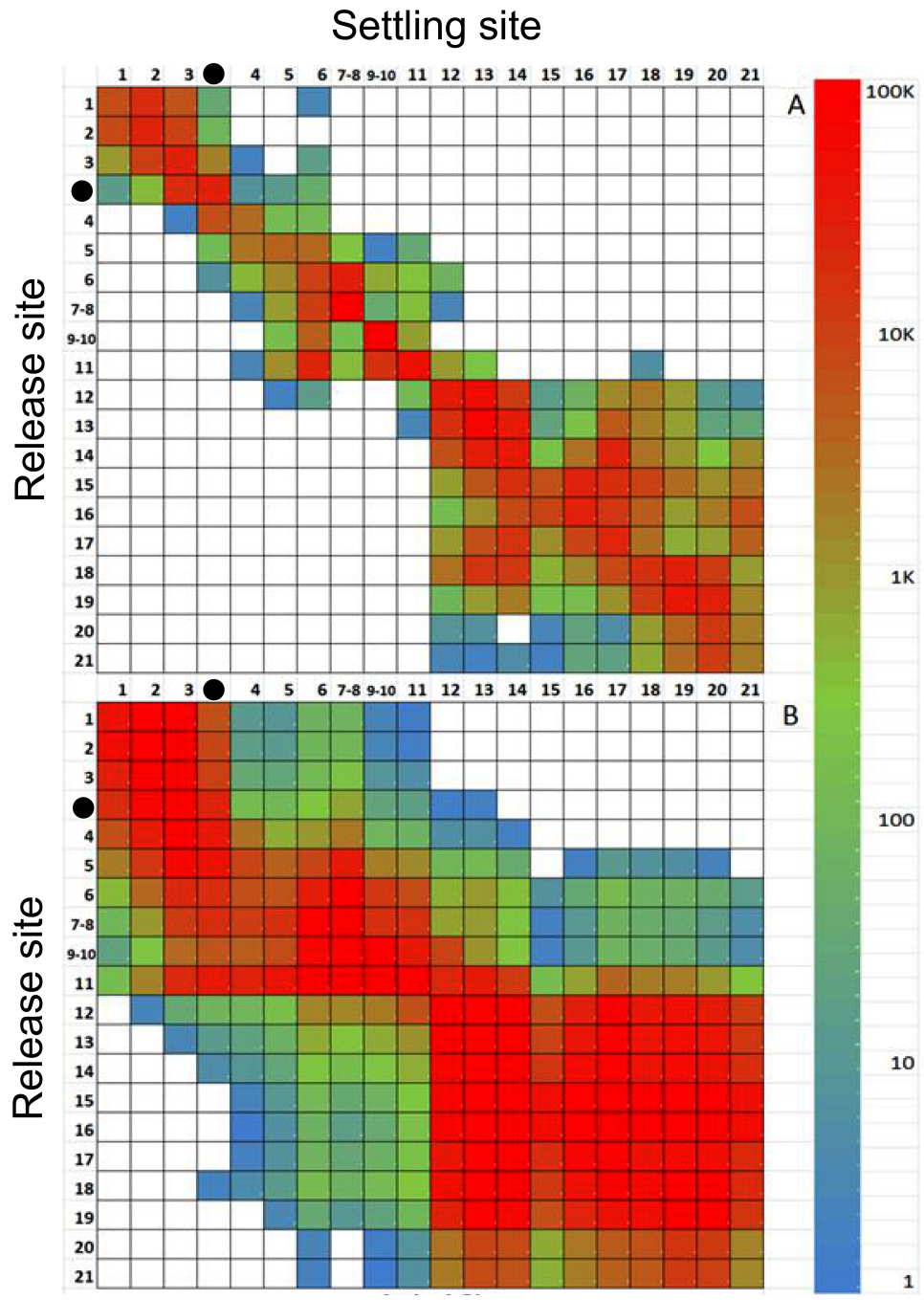

Fig. S4. Matrices of advection connectivity among 20 sites along the temperate coast of Australia; Model 1 (panel A): particles were advected from 30 to 150 days; Model 2 (panel B): stepping stone dispersal (four spawning cycles were considered, each with the same advection time as in Model 1). The black dot represents a site in the inaccessible GAB from which no genetic data were available, and two sites each in Spencer Gulf (sites 7 and 8) and Gulf St Vincent (sites 9 and 10) were merged.

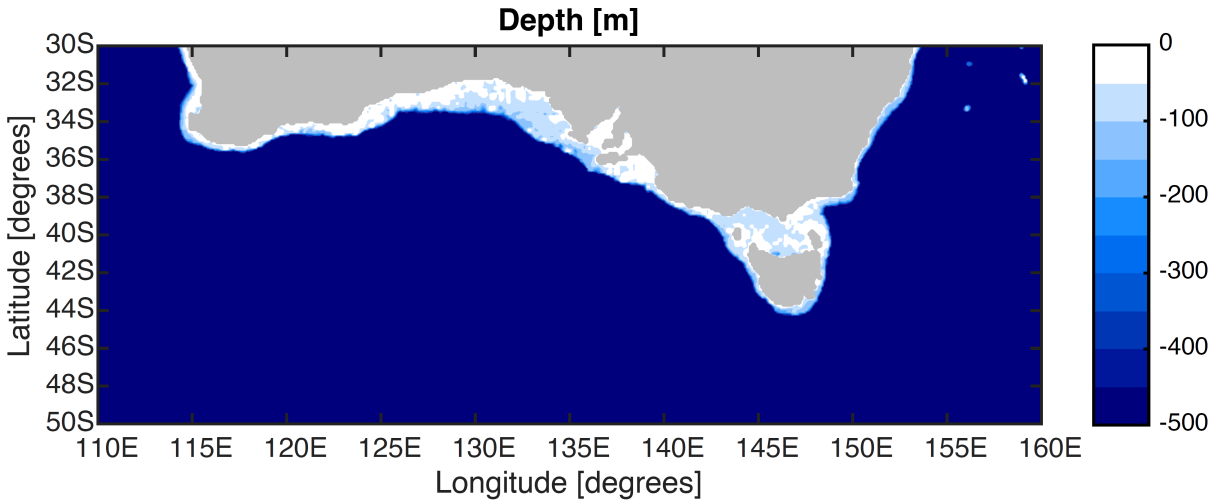

Fig. S5. Bathymetry of southern Australia. The region beyond the shelf edge is shown in dark blue.

Supplement 4: Accompanying information on the animation depicting dispersal of propagules from 20 sites along the Southern Australian coast

The animation is available at www.int-res.com/articles/suppl/m532p001_supp/

Each release site is uniquely coloured. The animation shows the dispersion of virtual particles in the OFES data for the season 1980/1981. One virtual particle is released from every site for every day between 1 September and 31 January, and is then integrated for 150 days.

At sites 1-3 (LC regions), there was some evidence for eastward dispersal that was likely driven by the LC at the beginning of the spawning season, but for most of the time, particles dispersed over short distances along the coast. In the GAB region (sites 3-6), propagules dispersed very little during most of the spawning season, and only very late (January) was there evidence for westward dispersal, strong influx of propagules from South Australia, and some dispersal by means of offshore boundary flow. In South Australia (sites 6-11), gradual westward drift was observed, but most particles remained on the continental shelf. In the south-east, there was some movement of particles into the Bass Strait in the ZC region during September/October, but only short-distance dispersal near the coast during most of the remainder of the spawning season, and most particles released in the Bass Strait remained there rather than becoming entrained in the ZC or EAC.

Supplement 5: Supplementary References

Escudero A, Iriondo JM, Torres ME (2003) Spatial analysis of genetic diversity as a tool for plant conservation. Biol Conserv 113: 351–365

Masumoto Y, Sasaki H, Kagimoto T, Komori N, Ishida A, Sasai Y, Miyama T, Motoi T, Mitsudera H, Takahashi K, Sakuma H, Yamagata T (2004) A fifty-year eddy-resolving simulation of the world ocean – preliminary outcomes of OFES (OGCM for the Earth Simulator). J Earth Simulator 1:35–56

Paris CB, Helgers J, van Sebille E, Srinivasan A (2013) Connectivity modelling system: a probabilistic modelling tool for the multi-scale tracking of biotic and abiotic variability in the ocean. Env Model Soft 42:47–54

Schlitzer R (2002) Interactive analysis and visualization of geoscience data with Ocean Data View. Comput Geosci 28:1221–1218

Van Sebille E, England MH, Zika JD, Sloyan BM (2012) Tasman leakage in a fine-resolution ocean model. Geophys Res Lett 39: L06601